Significance of halogens (F, Cl) in kimberlite melts: Insights from mineralogy and melt inclusions in the Roger pipe (Ekati, Canada)

Adam Abersteiner[1], Vadim S. Kamenetsky[1], Maya Kamenetsky[1], Karsten Goemann[3], Kathy Ehrig[4], Thomas Rodemann[3]

[1] *School of Physical Sciences, University of Tasmania, Australia, adam.abersteiner@utas.edu.au, dima.kamenetsky@utas.edu.au, Maya.Kamenetsky@utas.edu.au*

[2] *Central Science Laboratory, University of Tasmania, Australia, Karsten.Goemann@utas.edu.au, Thomas.Rodemann@utas.edu.au*

[3]*BHP Billiton Olympic Dam, Adelaide, Australia, Kathy.J.Ehrig@bhpbilliton.com*

Introduction

The abundance and distribution of halogens (F, Cl) are rarely recorded in kimberlites and therefore their petrogenetic significance is poorly constrained. Halogens are usually present in kimberlite rocks in the structure of phlogopite and apatite, but their original concentrations are never fully retained due to the effects of alteration. Fluorine and chlorine in magmatic systems are influential on melt viscosity, phase equilibria and the mobility of metals (Kamenetsky et al., 2007; Tropper and Manning, 2007; Brey et al., 2009). Therefore, elucidating the halogen content of kimberlite magmas is fundamental in understanding parental melt compositions, rheology and ultimately their petrogenesis.

In this study, we examine a sample of hypabyssal kimberlite from the Roger pipe (Ekati, Canada). A remarkable feature of the Roger kimberlite is the presence of F-bearing minerals (i.e. bultfonteinite: $Ca_4(Si_2O_7)(F,OH)_2$ and fluorite) replacing olivine. In order to constrain the evolution of kimberlite melts and the origin of halogens in the Roger kimberlite, we focus on documenting the petrography and geochemistry of halogen-bearing minerals and characterise melt inclusions hosted within olivine and magmatic groundmass minerals.

Petrography and Geochemistry

The studied sample is characterised by porphyritic textures defined by euhedral-to-anhedral olivine set in a fine-grained groundmass consisting largely of interstitial serpentine, carbonate (i.e. calcite) and to a lesser extent garnet (andradite-schlorlomite). The groundmass mineralogy is typical of hypabyssal Group-I (or archetypal) kimberlites (Mitchell, 1986, 2008) and contains abundant monticellite (~20 vol.%) along with subordinate amounts of phlogopite, apatite, Fe-Mg-Al-Cr-spinel (i.e. magnesian ulvöspinel-magnetite (MUM), Mg-magnetite, pleonaste, Cr-spinel), perovskite and Ni ± Fe-sulphides.

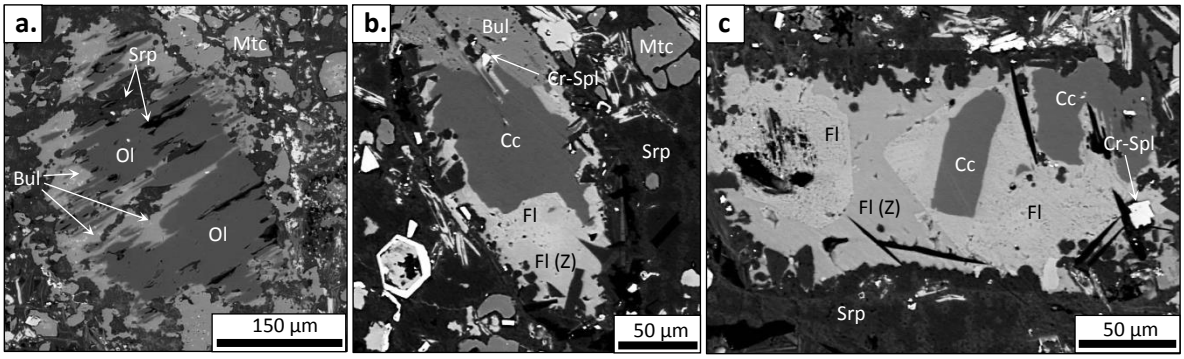

Figure 1. Back-scattered electron (BSE) SEM images of (a – c) Olivine (Ol) showing varying degrees of replacement by fluorite (Fl), bultfonteinite (Bul), serpentine (Srp) and calcite (Cc). (b, c) Pseudomorphic fluorite is zoned where darker fluorite areas are characterised by O-enrichment (Fl (Z)) and lighter fluorite areas contain minor-O (Table 1). Mtc: monticellite, Cr-Spl: Cr-spinel.

Bultfonteinite and fluorite are common replacement minerals after olivine which also overprint secondary calcite replacing olivine (Fig. 1) as well occurring as rare interstitial segregations (up to ~125 µm) throughout the groundmass. Bultfonteinite is homogeneous in composition, whereas fluorite is usually irregularly zoned along crystal faces in contact with the groundmass (i.e. rims) which is characterised by F-depletion and O-enrichment (Fig. 1c; Table 1). This abundance of F-rich minerals in the Roger kimberlite is illustrated by F-content (2263 and 2688 ppm). These results are consistent with previous analyses (1534 – 2532 ppm F; Nowicki et al., 2008) of the Roger kimberlite.

	Bultfonteinite					Fluorite			
	1	**2**	**3**	**4**		**4-R**	**5-R**	**13-C**	**8-C**
SiO_2	28.11	28.27	29.13	28.06	**Si**	0.27	0.23	0.03	0.09
FeO	0.51	0.14	0.15	0.64	**Fe**	0.18	0.12	0.05	0.14
MgO	0.28	<0.02	<0.01	0.20	**Mg**	0.04	0.06	<0.01	<0.01
CaO	52.41	53.07	51.57	52.30	**Ca**	48.14	47.87	50.62	50.1
SO_3	0.44	<0.01	0.01	0.52	**Sr**	0.23	0.32	0.22	0.31
F	8.87	9.26	9.20	9.36	**Na**	0.10	0.10	0.07	<0.02
H_2O	12.91	12.77	12.90	12.78	**F**	43.76	43.03	47.20	47.00
-O=F	3.73	3.90	3.87	3.94	**O**	7.21	7.75	0.95	1.46
Total	99.79	99.61	99.10	99.91	**Total**	99.93	99.48	99.14	99.11

Table 1. Representative mineral analyses of bultfonteinite and fluorite replacing olivine in oxide and element wt.% respectively. R = rim, C = core.

Inclusions

In order to examine the composition and evolution of the kimberlite melt prior to post-magmatic processes, we analysed melt inclusions in olivine, Cr-spinel, monticellite and apatite using a scanning electron mincroscope (SEM). Inclusions in Cr-spinel, monticellite and apatite contain polycrystalline assemblages, are randomly distributed throughout their host grain and located away from any fracture system, and are therefore considered to be primary. In contrast, olivine hosted inclusions are located along internal healed fractures and are therefore interpreted to be secondary, as defined by Roedder (1984). Melt inclusions contain heterogeneous daughter phase assemblages (Fig. 2) composed of alkali/alkali-earth (Na, K, Ba, Sr)-enriched Ca-Mg-carbonates ± F/V, Na-K-chlorides and sulphates, phosphates, spinel, silicates (e.g. olivine, phlogopite, (clino)humite) and sulphides. In addition, melt inclusions also contain other 'exotic' phases which include Ba-K ± W ± V ± Mo-bearing phases, alkali-REE-phosphates and scheelite.

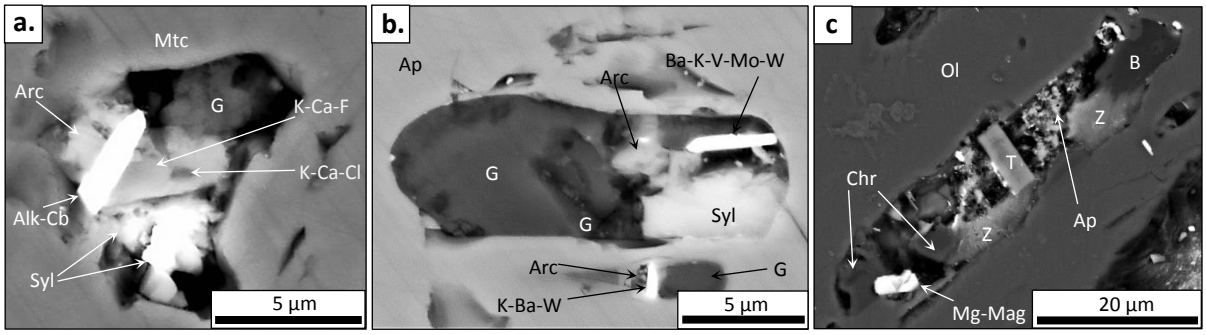

Figure 2. Back-scattered electron (BSE) SEM images of multiphase inclusions in: (a) monticellite (Mtc), (b) apatite (Ap) and (c) olivine. These multiphase inclusions host daughter phases of: gregoryite (G: $(Na_2,K_2,Ca)CO_3$), alkali-carbonate (Alk-Cb), arcanite (Arc: K_2SO_4), zemkorite (Z: $(Na,K)_2Ca(CO_3)_2$), tetraferriphlogopite (T: $KMg_3(Fe^{3+}Si_3O_{10})(OH)_2$), sylvite (Syl), Mg-magnetite (Mg-Mag), bradleyite (B: $Na_3Mg(PO_4)(CO_3)$), apatite (Ap),clinohumite (Chr)), Ba-K-V-Mo-W-phase (Ba-K-V-Mo-W), K-Ca-F-bearing phase (K-Ca-F), Ka-Ca-Cl-bearing phase (K-Ca-Cl) and K-Ba-W-bearing phase.

The Roger kimberlite is unique amongst other Ekati kimberlites, as it contains the highest F-content (up to 2688 ppm) and large amounts of F-rich minerals (i.e. bultfonteinite, fluorite) replacing olivine. The compositions and textures of bultfonteinite and fluorite in the Roger kimberlite are consistent with a secondary origin. The formation of interstitial andradite-schlorlomite garnet is indicative of hydrothermal precipitation from a Ca-bearing hydrothermal serpentinising fluid (Stripp et al., 2006; Buse et al., 2010). In addition, based on the occurrence of bultfonteinite and fluorite, it is inferred that this alteration fluid was also F-bearing. Buse et al. (2010) constrained the temperature range for secondary hydrogarnet and bultfonteinite formation in basalt xenoliths from the B/K9 kimberlite (Botswana) to occur between 350 – 250 °C, which is a similar temperature range to when serpentinisation occurs (Evans, 2004; Stripp et al., 2006; Mitchell, 2008). Therefore, it is likely the observed alteration assemblages in our sample formed at similar low-temperature conditions.

Comparisons between halogens and other trace elements of similar compatibility (i.e. F/Nd and Cl/U) in the Roger kimberlite and their respective estimated primitive mantle abundances show that halogens should be a more significant component in kimberlites than typically measured. We propose that fluorine in the Roger kimberlite was magmatic and was redistributed during hydrothermal alteration by Ca-bearing serpentinising fluids to produce the observed bultfonteinite/fluorite assemblages. The absence of alkali, halogen and other highly incompatible trace element bearing phases from the Roger groundmass and other kimberlites worldwide is attributed to alkalis and chlorine accommodated in water soluble phases (i.e. alkalis in carbonates, sulphates and phosphates, and Cl in chlorides). The scarcity of these components in the kimberlite groundmass is attributed to the near ubiquitous effects of syn- and post-magmatic alteration.

Based the compositions and daughter mineral assemblages in primary melt inclusions and reconstructed halogen abundances, we suggest that Cr-spinel, monticellite and apatite crystallised from a variably differentiated Si-P-Cl-F-bearing carbonate melt enriched in alkalis/alkali-earths and highly incompatible trace elements. This presence of halogens in the parental kimberlite melt may bear unrecognised implications for melt liquidus temperatures, rheological properties and composition.

References

Brey GP, Bulatov VK, Girnis AV (2009) Influence of water and fluorine on melting of carbonated peridotite at 6 and 10 GPa. Lithos 112:249-259.

Buse B, Schumacher J, Sparks RSJ, Field M, (2010) Growth of bultfonteinite and hydrogarnet in metasomatized basalt xenoliths in the B/K9 kimberlite, Damtshaa, Botswana: insights into hydrothermal metamorphism in kimberlite pipes. Contrib Mineral Petrol 160:533-550.

Evans B (2004) The Serpentinite Multisystem Revisited: Chrysotile Is Metastable. Int Geol Rev 46: 479-506.

Kamenetsky, VS, Kamenetsky, MB, Sharygin, VV, Golovin, AV (2007) Carbonatechloride enrichment in fresh kimberlites of the Udachnaya-East pipe, Siberia: a clue to physical properties of kimberlite magmas? Geophys. Res. Lett. 34.

Mitchell RH (1986) Kimberlites: Mineralogy, Geochemistry and Petrology. Plenum Publishing Company, New York, 442 pp.

Mitchell RH (2008) Petrology of hypabyssal kimberlites: Relevance to primary magma compositions. J Volcanol. Geotherm Res 174:1-8.

Nowicki T, Porritt L, Crawford,B, Kjarsgaard B (2008) Geochemical trends in kimberlites of the Ekati property, Northwest Territories, Canada: Insights on volcanic and resedimentation processes. J Volcanol Geotherm Res 174:117-127.

Stripp GR, Field M, Schumacher JC, Sparks RSJ, Cressey G (2006) Post-emplacement serpentinization and related hydrothermal metamorphism in a kimberlite from Venetia, South Africa J Metamorph Geol 24:515-534.

Tropper P, Manning CE (2007) The solubility of fluorite in H_2O and H_2O–NaCl at high pressure and temperature. Chem Geol 242:299-306.